Collimated Electron Jets by Intense Laser-Beam–Plasma Surface Interaction under Oblique Incidence

H. Ruhl*
Theoretische Quantenelektronik, TU Darmstadt, Hochschulstrasse 4A, 64289 Darmstadt, Germany

Y. Sentoku,[1,†] K. Mima,[1] K. A. Tanaka,[2] and R. Kodama[1]
[1]*Institute of Laser Engineering, Osaka University, 2-6 Yamada-oka, Suita Osaka, 565, Japan*
[2]*Department of Electromagnetic Energy Engineering and Institute of Laser Engineering, Osaka University, 2-6 Yamada-oka, Suita Osaka, 565, Japan*
(Received 16 July 1998)

Oblique incidence of a p-polarized laser beam on a fully ionized plasma with a low density plasma corona is investigated numerically by particle-in-cell and Vlasov simulations in two dimensions. A single narrow self-focused current jet of energetic electrons is observed to be projected into the corona nearly normal to the target. Magnetic fields enhance the penetration depth of the electrons into the corona. A scaling law for the angle of the ejected electrons with incident laser intensity is given. [S0031-9007(98)08030-2]

PACS numbers: 52.40.Nk, 52.25.Dg, 52.65.–y

The availability of tabletop high intensity laser systems has led to the investigation of novel regimes of short pulse laser-plasma interaction. Recently the emission of collimated electron jets under specular angles with respect to the density normal direction has been observed for an obliquely incident laser beam on a steep density plasma [1].

When a target is irradiated by an intense laser pulse above the field ionization threshold it quickly ionizes [2]. For sufficiently long laser pulse irradiation, the plasma present on the surface gradually expands into the vacuum with the ion acoustic speed. Hence, a plasma corona is formed. For short laser pulses there is not enough time for hydrodynamic expansion. Short pulse simulations show, however, that an ion shelf is formed on a typical time scale $t_s = \omega_0^{-1}(m_i/Zm_e)^{1/2}$ due to the generation of a strong electric field at the plasma-vacuum interface [3]. This ion shelf represents a low density plasma corona.

There are different mechanisms which can lead to collimated electron jets when an intense laser pulse interacts with a vastly overdense, steep density plasma that has a low density plasma corona. One effect that plays a role in the interaction is the Brunel effect [4] which works for oblique incidence. Here the electrons are accelerated into the vacuum as well as into the target by the electric field present along the density gradient. The coronal plasma is expected to collimate and enhance the range of the ejected electrons in two (2D) or three (3D) spatial dimensions by quasisteady magnetic field generation. The collimating effect of quasisteady fields has recently been addressed in Refs. [5,6] in a different context.

To investigate the phenomenon just outlined in more detail we perform both particle-in-cell (PIC) and Vlasov (VL) simulations in two spatial dimensions. In both approaches we do not simulate the evolution of the corona self-consistently but treat it parametrically with ions fixed. In our PIC simulations we rotate the target, and in our VL simulations we boost to the frame of normal incidence to model oblique incidence of the laser beam. The boost frame method is well established in 1D [7–9]. However, in 2D using the boost frame is very helpful in establishing the physics of the underlying laser-plasma interaction.

We investigate the interaction of a p-polarized laser beam incident under angles of 30° (PIC) and 45° (VL) on a preformed fully ionized target with an underdense plasma corona in front of it. In both simulations the laser beam has a duration of about 100 fs. For the PIC case the laser beam intensity is 2.0×10^{18} W/cm^2 and for the VL case it is 1.0×10^{17} W/cm^2. The laser wavelength in the simulations is 1 μm with beam diameters of 8 μm (PIC) and 5 μm (VL) at full width at half maximum. The coordinates of the simulation box are x and y, respectively. The size of the simulation box is 23 μm $\times$ 23 μm for the PIC simulations and 6 μm $\times$ 12 μm for the VL simulations. In our PIC simulations we assume mirror-reflecting boundary conditions for the electrons in x and y directions. In the VL simulations we use periodic boundary conditions in the y direction. Electrons leaving the simulation box at $x = 6$ μm are replaced by thermal electrons and at $x = 0$ μm they are allowed to escape. We note that mirror-reflecting boundary conditions in our PIC simulations force us to increase the simulation box for long simulation times. The distribution functions for the electrons and ions needed for the VL simulations have, in addition, two momentum directions p_x and p_y. The quasiparticle number per cell used in the PIC simulations is 50 for each species. The fully ionized plasma density is $4n_c$ (PIC) and $8n_c$ (VL). In both simulations we assume a uniform low density plasma corona with a density of $0.1n_c$ in front of the target.

Plot (a) of Fig. 1 gives the quasisteady magnetic field B_z in front of the target inclined at 30°, as obtained by PIC

simulations. The peak magnitude of the normalized magnetic field is 0.62, which corresponds to approximately 30 MG . It changes polarity very rapidly along the density gradient revealing the presence of a very localized self-focused current jet. The low density plasma corona guarantees quasineutrality and helps to generate the magnetic field in front of the target. Figure 1(b) shows the electron energy density. We find a collimated electron jet which coincides with the quasisteady magnetic field from Fig. 1(a). For the parameters of Fig. 1(b) the ejection angle is approximately 17° from the target normal. There are also fast electrons injected into the overdense plasma. We again observe that they are almost normal to the target surface. Figure 1(c) shows the instantaneous plot of the electron energy density with the overplotted positive B_z field indicating the phase of the laser field. It is clearly seen that the outgoing electrons are generated on the target surface once per laser cycle by the Brunel absorption mechanism [4,8] and are, consequently, bunched on the scale of the laser wavelength. The range of the electrons is enhanced. We obtain a similar result from our VL simulations which make use of boost frame coordinates.

To illustrate how the boost frame approach for oblique incidence in 2D works we briefly derive the correct boundary conditions for the laser pulse in the boosted frame. We start by defining an arbitrary pulse envelope function $z(x, y, t)$ in the lab frame. Next we perform a Lorentz rotation of electromagnetic fields about (x_0, y_0). In the final step we boost the latter to the frame of normal incidence for which the longitudinal field E_x disappears. We obtain

$$E_x^B = 0, \qquad E_y^B = \frac{1}{\bar{\gamma}}\, z(x_r, y_r, t)\,, \qquad B_z^B = \frac{1}{c\bar{\gamma}}\, z(x_r, y_r, t)\,, \tag{1}$$

where

$$x_r = \frac{1}{\bar{\gamma}}\,(x - x_0) + (y - y_0)\bar{\beta}, \qquad y_r = \frac{1}{\bar{\gamma}}\,(y - y_0) - (x - x_0)\bar{\beta}\,, \tag{2}$$

with

$$t = \frac{\bar{\gamma}\bar{\beta}}{c}\, y^B, \qquad x = -ct^B, \qquad y = \bar{\gamma} y^B. \tag{3}$$

The function z is the same function as in the lab frame. For the relativistic factors we have $\bar{\beta} = \sin\theta$ and $\bar{\gamma} = 1/\cos\theta$, where θ is the angle of incidence. Plot (a) of Fig. 2 illustrates the incident time resolved electromagnetic field E_y for a Gaussian pulse envelope. Figure 2(b) gives the incident time-resolved electromagnetic field E_y of the simulations.

Plot (a) of Fig. 3 gives the quasisteady magnetic field in the plasma corona in front of the overdense plasma target. Figure 3(b) gives the quasisteady magnetic field with the quasisteady B_z^2 overplotted (red solid lines). Figure 3(c) gives the quasisteady magnetic field with the quasisteady longitudinal current density j_{xe} overplotted (red dashed lines).

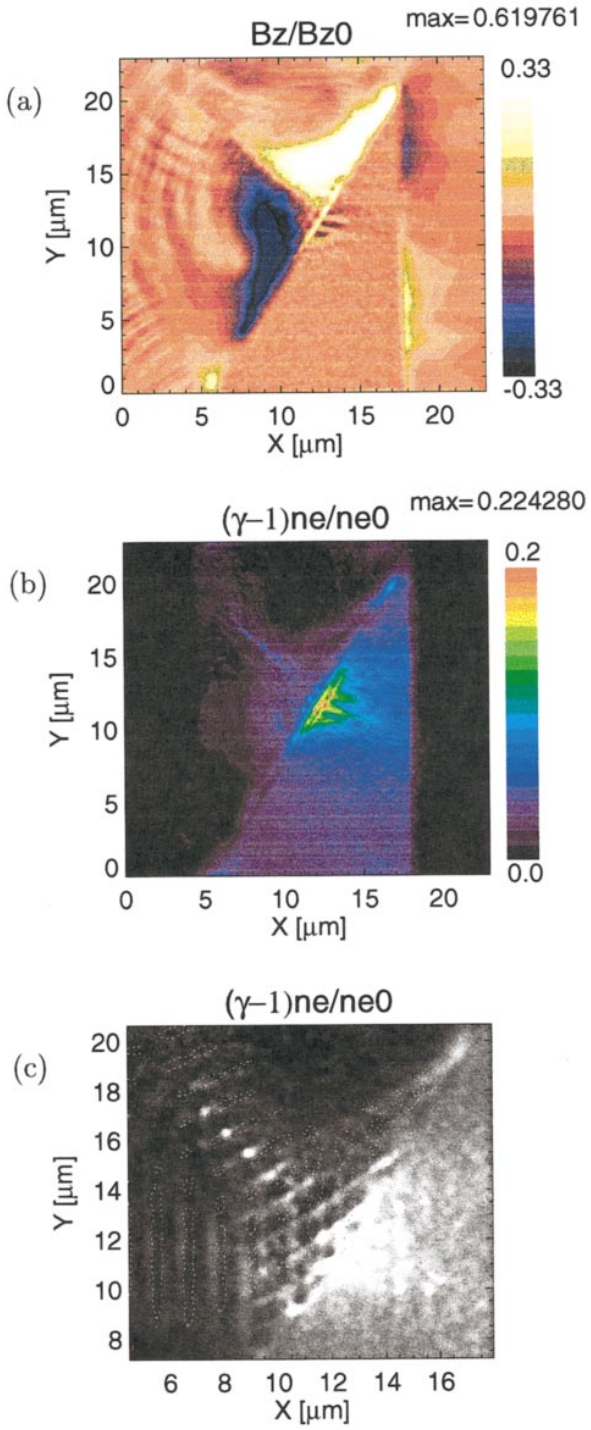

FIG. 1(color). Quasisteady magnetic field B_z (a); quasisteady electron energy density ϵ (b); and instantaneous electron energy density with the laser field B_z (c). Yellow contour areas are positive and blue areas are negative. The parameters are $n/n_{\text{crit}} = 4$, $I\lambda^2 = 2.0 \times 10^{18}$ W cm^{-2} μm^2, $\theta = 30°$, $t = 120$ fs, and $B_{z0} = 100$ MG.

Since the current density j_{xe} is invariant under Lorentz boosts along y it may serve as a quantity from which to

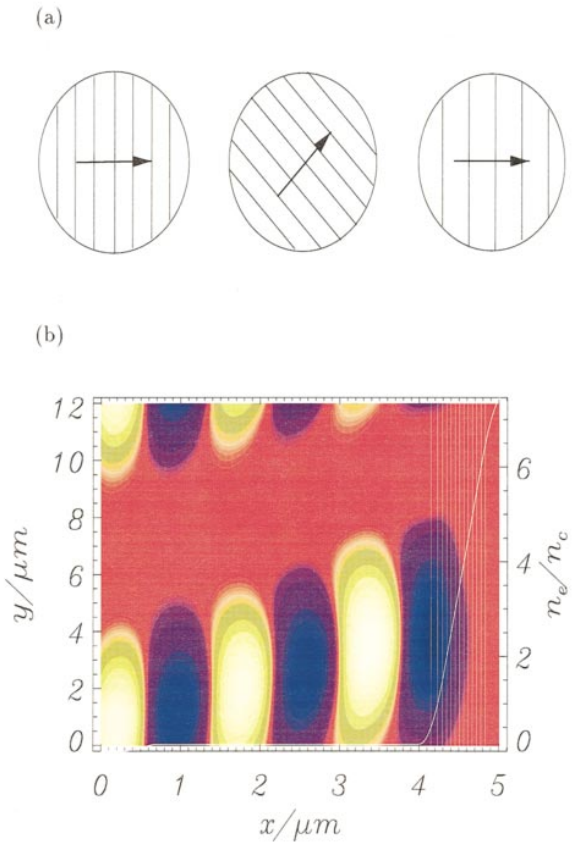

FIG. 2(color). Illustration of the boost technique in 2D for an incident laser pulse of Gaussian pulse envelope (a) and time resolved E_y taken in the simulations (b). The left figure in (a) gives the incident pulse, the figure in the middle gives the pulse after a rotation, and the right figure shows the pulse after the final boost. The arrows in (a) indicate the propagation direction of the laser pulse. The white solid lines in (b) give the density profile. The parameters for (b) are $n/n_{\rm crit} = 8$, $I\lambda^2 = 1.0 \times 10^{17}$ W cm^{-2} μm^2, $\theta = 45°$, and $t = 25$ fs.

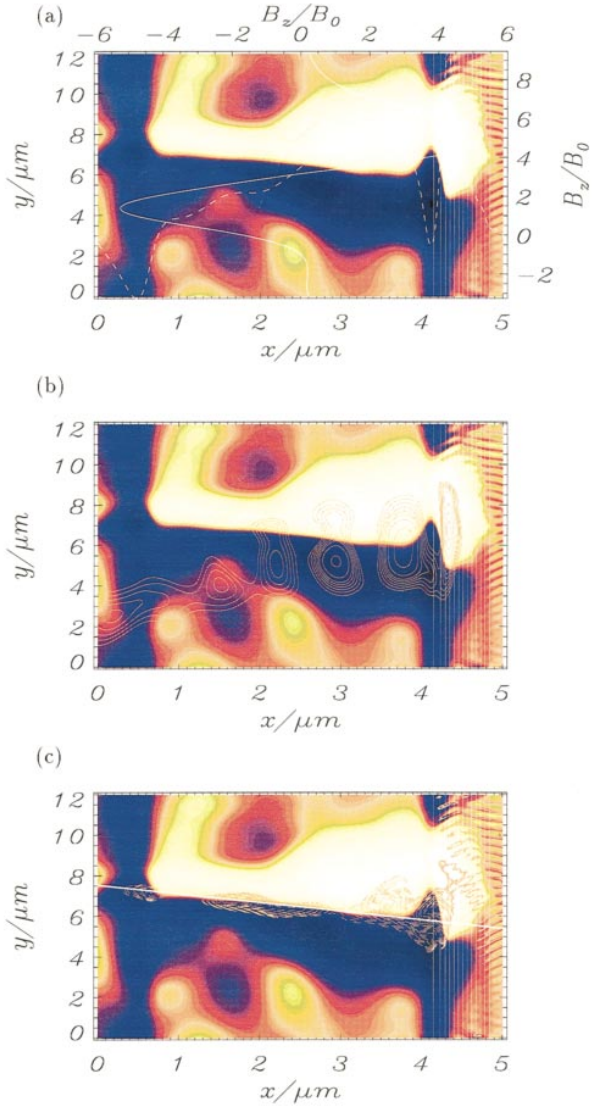

FIG. 3(color). Quasisteady B_z (a); quasisteady B_z with quasisteady B_z^2 overplotted (b); and quasisteady B_z with current density overplotted (c). Yellow contour areas are positive and blue areas are negative. The white solid lines along y located between $x = 4$ μm and $x = 5$ μm are density isocontours. The other lines overplotted in (a) indicate the quasisteady magnetic field. They are along $x = 3.63$ μm (solid line) and $y = 7.18$ μm (dashed line). The parameters are $n/n_{\rm crit} = 8$, $I\lambda^2 = 1.0 \times 10^{17}$ W cm^{-2} μm^2, $\theta = 45°$, $t = 75$ fs, and $B_0 = 1.5$ MG.

determine the direction of the electron jets. We now introduce the coordinates $\chi = x^B$ and $\xi = y^B + \bar{\beta} c t^B$ which move along with the background plasma current present in the boosted frame. Since the time-averaged current density $\langle j_{xe}^B \rangle$ in the comoving coordinates varies slowly with time, we obtain $\langle j_{xe}^B \rangle (x^B, y^B, t^B) = \langle j_{xe}^B \rangle (\chi, \xi)$. This yields

$$\langle j_{xe}^L \rangle (\chi, \xi) = \langle j_{xe}^B \rangle (\chi, \bar{\gamma}\xi). \quad (4)$$

The direction of the collimated electron jets in the lab frame can now be calculated from the direction of the current density in the boosted frame. Figure 3(c) gives $\langle j_{xe}^B \rangle$. The direction of the emitted electrons is indicated by the white solid line plotted in the figure. We obtain a mean emission angle of 20° in the boosted frame and 14° in the lab frame. We note that the lab frame is dilated in transverse direction when viewed from the boosted frame, and hence the emission angle in the boost frame is larger by a factor of $\bar{\gamma} = 1/\sqrt{1 - \bar{\beta}^2}$ as indicated by Eq. (4).

In boost frame coordinates we may easily analyze the physical mechanism that leads to the large areal quasisteady magnetic field and the direction of the ejected electrons. We recall that in the boosted frame we have a constant background fluid velocity $u_B = c \sin\theta$ which approaches the speed of light for large angles of incidence. In this frame the polarization of the magnetic field vector of the incident laser beam is normal to the xy plane and to the flow direction of the background current. If the laser intensity is small enough as in [1] and the angle of incidence sufficiently large the boost velocity exceeds the laser quiver velocity. The driving force under these conditions is exerted predominantly by the oscillating magnetic field of the laser beam [see the

red solid contour lines of B_z^2 plotted over B_z in Fig. 3(b) for the location of the force]. The resulting force is $\mathbf{F} = -e\mathbf{u}_B \times \mathbf{B}$ and is capable of ejecting electrons out of the surface at a rate of one per laser cycle. This is the Brunel mechanism [4]. The quasisteady magnetic field in the plasma corona is generated by the electron current emitted from the target. The polarization of the magnetic field is such that it collimates the electrons propagating through the plasma corona.

To derive an approximate criterion for the angle range under which the fast electrons are emitted from the target surface we assume that the laser target interaction in the boosted frame is quasi-one-dimensional. Since the full width at half maximum of the laser beams in our simulations is at least 5 μm and the intensities are sufficiently low to prevent target imprinting, we believe that this assumption is justified. We next rewrite the Vlasov equation in the boosted frame [10] and solve it for an initial Maxwellian. We approximate the plasma-vacuum interface by a steplike density profile with $n(x) = n_0$ for $x > 0$ and treat the ions as immobile. We obtain for the distribution function

$$f(t) = \frac{n_0}{\sqrt{2\pi}m^3 v_{th}^3 3} \exp\left(-\frac{p_x^2(0) + p_z^2(0)}{2m^2 v_{th}^2}\right) \times \exp\left(-\frac{(p_y(0) + \bar{\beta}\bar{\gamma}mc)^2}{2\bar{\gamma}^2 m^2 v_{th}^2}\right), \quad (5)$$

and for the equations of motion

$$x(\tau) = x - \int_\tau^t d\eta\, v_x(\eta), \quad (6)$$

$$p_x(\tau) = p_x + e\int_\tau^t d\eta [E_x(x(\eta),\eta) + v_y(\eta)\partial_x A_y(x(\eta),\eta)], \quad (7)$$

$$p_y(\tau) = p_y + e[A_y(x(\tau),\tau) - A_y(x,t)], \quad (8)$$

$$p_z(\tau) = p_z, \quad (9)$$

with

$$v_{x/y}(\tau) = \frac{c p_x(\tau)}{\sqrt{m^2c^2 + p_x^2(\tau) + p_y^2(\tau) + p_z^2(\tau)}}. \quad (10)$$

Equations (8) and (9) indicate lateral canonical momentum conservation in boost frame coordinates. We now assume that A_y has a harmonic time dependence. Making use of Eqs. (5) and (8) and assuming $v_x \ll c$ or $v_x \approx c$, we obtain $\langle p_y\rangle \approx -\bar{\beta}\bar{\gamma}mc$. The quantity $\langle p_y\rangle$ denotes the ensemble and time-averaged transverse momentum. Treating $\langle p_x\rangle$ as a free parameter and transforming back to the lab frame yields

$$\langle p_y^L\rangle = \bar{\gamma}^2\bar{\beta}mc(\sqrt{1 + \langle p_x^2\rangle/\bar{\gamma}^2m^2c^2} - 1), \quad \langle p_x^L\rangle = \langle p_x\rangle. \quad (11)$$

The ejection angle is now given by $\tan\theta' = \langle p_y^L\rangle/\langle p_x^L\rangle$. For $\langle p_x\rangle \to \infty$ we obtain $\tan\theta' = \bar{\beta}\bar{\gamma} = \tan\theta$. This means that only ultrarelativistic electrons are ejected at very close to specular direction. For smaller longitudinal momenta $\langle p_x\rangle$, we expect that the electrons are emitted at angles that are smaller than the angle for specular emission as observed in our simulations. Assuming that the mean fast electron momentum in x direction is given by $\langle p_x\rangle/\bar{\gamma}mc \approx \sqrt{\alpha I\lambda^2}$, we thus obtain

$$\tan\theta' = \frac{\sqrt{1 + \alpha I\lambda^2} - 1}{\sqrt{\alpha I\lambda^2}} \tan\theta. \quad (12)$$

Equation (12) loses validity as soon as target deformations start to become significant. The validity also depends on the accuracy of the mean longitudinal momentum given as a function of intensity. For $I\lambda^2 = 1.0 \times 10^{17}$ W cm^{-2} μm^2 we obtain an ejection angle of $\theta' = 14°$, and for $I\lambda^2 = 2.0 \times 10^{18}$ W cm^{-2} μm^2 we obtain $\theta' = 17°$ from the simulations. This yields $\alpha^{-1} \approx 8.0 \times 10^{17}$ W cm^{-2} μm^2.

In conclusion, we have demonstrated, with the help of two different simulation techniques, that collimated electrons with enhanced range can be emitted from an overdense target if a low density plasma corona is present. In addition, we have shown that fast electrons are injected into the overdense plasma. Both the ejection and the injection directions are almost along the density normal direction for p-polarized light. By a transformation to the moving frame in which the laser pulse appears to be normally incident, we were able to give a criterion for the angle range of the emitted electrons with ejection momentum. We find that, for a planar interaction interface, only speed-of-light electrons can be emitted at specular direction for p-polarized light. Less energetic electrons appear under almost normal emission angles due to a lack of lateral momentum transfer. This analytical result is in qualitative agreement with our numerical observations. We note that in addition to the mechanism outlined in this paper other mechanisms of fast electron generation, such as wake-field acceleration in the corona, may exist, leading to different emission angles.

*Electronic address: Hartmut.Ruhl@physik.th-darmstadt.de
†Electronic address: sentoku@ile.osaka-u.ac.jp

[1] S. Bastiani *et al.*, Phys. Rev. E **56**, 7179 (1997).
[2] D. Bauer *et al.*, Phys. Rev. E **58**, 2436 (1998).
[3] Paul Gibbon, Phys. Rev. Lett. **73**, 664 (1994).
[4] F. Brunel, Phys. Rev. Lett. **59**, 52 (1987).
[5] L. Gorbunov *et al.*, Phys. Plasmas **4**, 4358 (1997).
[6] A. Pukhov and J. Meyer-ter-Vehn, Phys. Rev. Lett. **79**, 2686 (1997).
[7] A. Bourdier, Phys. Fluids **26**, 1804 (1983).
[8] H. Ruhl and P. Mulser, Phys. Lett. A **205**, 388 (1995).
[9] Paul Gibbon, Phys. Rev. Lett. **73**, 664 (1994).
[10] H. Ruhl and A. Cairns, Phys. Plasmas **4**, 2246 (1997).